Relation between Velocity Profile and Friction Factor at High Reynolds Number in Fully Developed Pipe Flow

Noriyuki Furuichi and Yoshiya Terao
National Metrology Institute of Japan
National Institute of Advanced Industrial Science and Technology.
1-1-1 Umezono, Tsukuba, 305-8563, Japan
furuichi.noriyuki@aist.go.jp, terao.yoshiya@aist.go.jp

Yuki Wada and Yoshiyuki Tsuji
Department of Engineering
Nagoya University
Furo-cho, Chikusa-ku, Nagoya, Aichi 464-8603, Japan
wada-yuki11@ees.nagoya-u.ac.jp, c42406@cc.nagoya-u.ac.jp

ABSTRACT

The new experimental data of the fully developed pipe flow using Hi-Reff at AIST, NMIJ is presented. The experiments was performed at higher Reynolds number region up to 10^7. The velocity profile data was fitted to a velocity profile formula based on the log law, and an equation for the friction factor was derived by integration, which agreed very well with the friction factor data obtained from pressure drop and flowrate. The deviation between the derived equation and the measured friction factor data is less than 1%, which indicates the high reliability of the measurement data at the Hi-Reff.

INTRODUCTION

A pipe flow, which is one of the wall-bounded flows, is widely used in engineering fields. Since obtaining the knowledge of the physics of the pipe flow is very important for the fluid transportation, many works for the turbulent pipe flow under fully developed have been performed since early time of 1900's. However, even the functional form for the mean velocity profile is still not complete due to the Reynolds number effect. As summarized by Nagib and Shauhan (2008), the mean velocity profile form are not consistent among many previous studies (ex; den Toonder and Nieuwstadt, 1997, Zagarola and Smits, 1998, Monty, 2005).

One of the reason for the inconsistency of the velocity profile formulae is that the wall shear stress used for the scaling of the velocity profile is also inconsistent among the experiments. To obtain the wall shear stress of not only the pipe flows but also wall-bounded flows, the friction factor is very important. As well known, the Prandtl equation, which is given by the fitting to the experimental data by Nikradse (1966), has been accepted widely and for long time. On the other hand, as recent result at higher Reynolds number, Zagarolla and Smits (1998) presented the data for the friction factor and a new equation. The new equation is largely deviated from the Prandtl equation especially at higher Reynolds number. However, other experimental results for higher Reynolds number region cannot be found in previous reports.

The second reason of the inconsistency is the Reynolds number dependency of the velocity profile formula. As investigated in other type of the wall bounded flows, boundary layer and channel flow, the constants in the velocity profile formula are influenced by Reynolds number (Nagib and Shauhan, 2008). To discuss the universality of the velocity profile, the pipe flow experiments at higher Reynolds number region is required.

In this paper, the new experimental results for the friction factor and the velocity profile at high Reynolds number up to 10^7 are presented. The Reynolds number dependency of the constants in the formulae of the friction factor and the velocity profile are discussed using the experimental result. Furthermore, to show the reliability of the experimental results, the higher level consistency of the measurement data between the friction factor and velocity profile is presented.

EXPERIMENTAL METHOD

Experimental Facility

In this experiments, the Hi-Reff (High Reynolds number actual flow facility) at NMIJ, AIST was used (Furuichi et al, 2009). The Hi-Reff is illustrated in Fig.1. The scale of this facility is 200 m × 50 m length including the over flow head tank with 30 m height and the reservoir tank with 1000 t. This facility serves the national standard of water flowrate in Japan. The working fluid is water. Regarding the general specifications of this facility, the maximum flow rate in the test section is 3.33 m^3/s, and the temperature is controllable from 20 °C to 75 °C. The available pipe diameter is up to 600 mm. According to this flow condition, the maximum Reynolds number is approximately 2.0×10^7. The flow rate is measured by the static gravimetric method or the reference flowmeters calibrated by the weighing tank. The uncertainty of the flow rate ranges from 0.060% to 0.10% with the coverage factor of k=2.

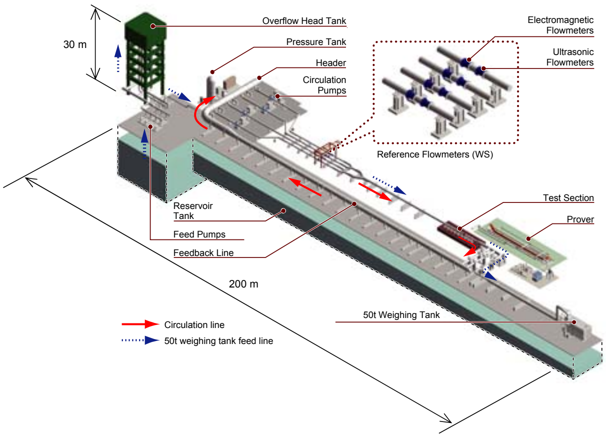

Figure 1. Overview of high Reynolds number actual flow facility (Hi-Reff).

Experimental Method

The friction factor is obtained by the measurement of the pressure drop between two pressure taps installed in smooth pipes with D = 100 mm (P1) and 387 mm (P2). The roughness of the pipes are Ra = 0.1 μm and 0.2 μm, respectively. The experiments are performed at two different temperatures: T=20 °C and 70 °C for P2. The examined Reynolds number range is $7.1\times10^3<Re_D<1.8\times10^7$. The uncertainty of the friction factor measurement is estimated to be app. 1.0% with a coverage factor of 2. In this paper, the data for $1.2\times10^4<Re_D<1.0\times10^7$ is used for the analysis.

The velocity profile was measured by using laser Doppler velocimetry (LDV). The water temperature is 20±1 °C and the examined Reynolds numbers are Re_D = 3.85×10^4, 7.33×10^4, 8.98×10^4, 1.49×10^5, 1.88×10^5, 2.84×10^5, 3.86×10^5, 5.40×10^5, 7.45×10^5, and 1.11×10^6. The control volume of the LDV system are 0.048 mm, 0.107 mm, and 0.40 mm for the streamwise, radius and tangential directions respectively. The spatial resolution in the y direction takes into account the inclination angle of the line for the measurement. The uncertainty of the velocity measurement is estimated to be 0.2% with a coverage factor of 2.

EXPERIMENTAL RESULT

Friction Factor

The experimental result of the friction factor λ is shown in Fig.2. The Reynolds number range examined is $7.1\times10^3<Re_D<1.1\times10^5$ for P1 and $4.7\times10^4<Re_D<1.8\times10^7$ for P2. As mentioned, the experiment is performed under two temperature conditions for P2. The Reynolds number ranges are $4.7\times10^4<Re_D<6.7\times10^6$ for T=20 °C and $3.3\times10^6<Re_D<1.8\times10^7$ for T=70 °C. Even though the present experiments are performed in different pipes and under different temperatures, the data plotted in the figure show smooth trends, and the scattering of the data is very small. In the overlapping Reynolds number ranges where the data from both pipes and both temperature conditions overlap, the deviation of the measured friction factors is less than 1%. This good agreement indicates the high reliability of the measurement result.

As the comparison with the results of the Superpipe, the present experimental results (McKeon et al,, 2004) show nice agreement with them for $Re_D<2.0\times10^5$. However, the difference between two results increases with Reynolds number for $Re_D>2.0\times10^5$. At $Re_D=1.0\times10^7$, the present experimental results is 6% smaller than the results of the Superpipe.

As the best fitting curve of the present experimental results, the following equation is given.

$$\frac{1}{\sqrt{\lambda}} = 2.092 \log\left(Re_D\sqrt{\lambda}\right) - 1.176 \qquad (1)$$

Note that the wall shear stress in the following section is obtained using the friction factor given by this equation. For more detail results, see reference (Furuichi et al., 2015).

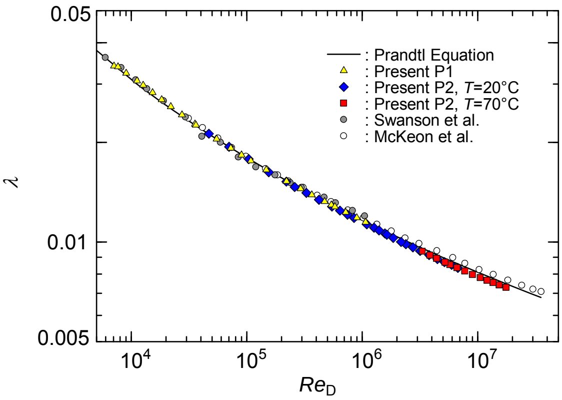

Figure 2. Experimental results for friction factor.

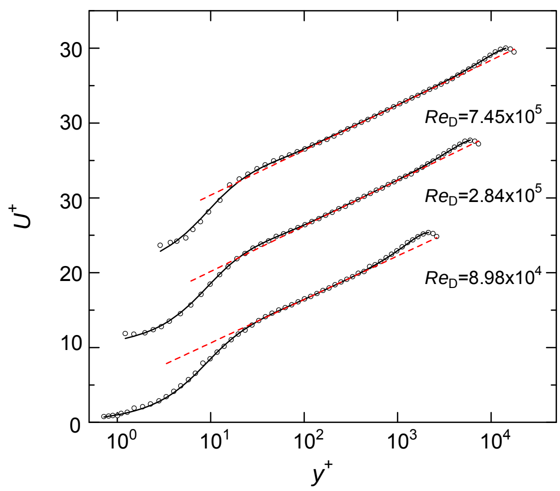

Figure 3. Examples of experimental results for velocity profile. The solid line is the fitting curve according to Musker equation.

Velocity Profile

The examples of the velocity profile obtained in this experiment are shown in Fig.3. The meaning of the several fitting curve indicated in Fig.3 will be explained in the following.

The general velocity profile based on the log-law is given by the following.

$$U^+ = \frac{1}{\kappa}\ln y^+ + B \tag{2}$$

where κ is Kármán **c**onstant and B is the additive constant. The both value obtained by each velocity profile is shown in Fig.4 and Fig.5. The both values have the Reynolds number effect. The Kármán constant is ranged from 0.39 to 0.40 for $Re_D<2.0\times10^5$ and it decreases suddenly at $Re_D\approx2.0\times10^5$. For the higher Reynolds number region, $Re_D>5.0\times10^5$, it takes almost constant value, which is 0.383. This results is different with results of the Superpipe, which is 0.41-0.42. On the other hand, this result shows nice agreement with the valued given in the recent results for the boundary layer and channel flow (Nagib and Shauhan, 2008). Considering with the canonical flow of the wall-bounded flow, such consistency is very interested.

The red broken lines in Fig.3 are Eq.(2) with κ and B as shown in Fig.4 and 5.

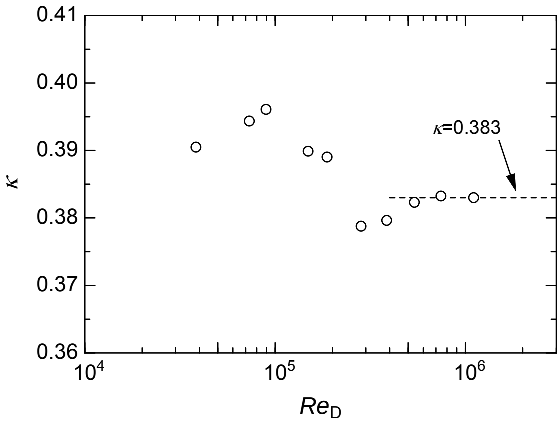

Figure 4. Variation of Kármán constant.

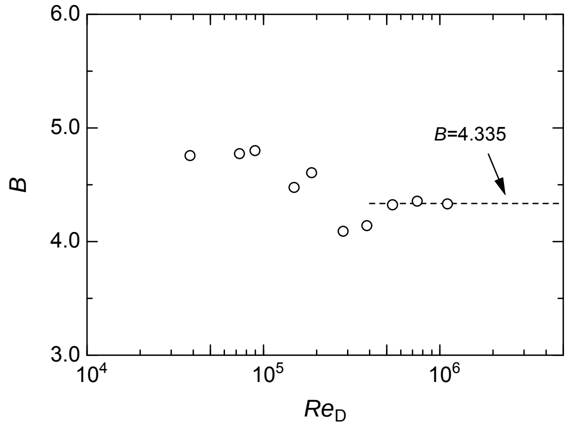

Figure 5. Variation of additive constant.

DISCUSSION

Velocity Profile Form

By integrating Eq.(2) over the pipe, the following relation for the friction factor is obtained.

$$\frac{1}{\sqrt{\lambda}} = \frac{1}{2\kappa\sqrt{2}}\ln\left(Re_D\sqrt{\lambda}\right) + \frac{B}{2\sqrt{2}} - \frac{1}{2\kappa\sqrt{2}}\left\{\frac{3}{2} + \ln\left(4\sqrt{2}\right)\right\} \tag{3}$$

According to this equation, κ and B in Eq.(1) is calculated to be 0.389 and 4.984, respectively. These values should be consistent between the velocity profile and friction factor. In other words, the consistent values indicate the validity of the measurement result. Unfortunately, these values are not consistent with the result of the velocity profile. This inconsistency is firstly from that Eq.(3) does not include the viscous sublayer and the wake. Then, to derive the equation for the friction factor and to compare it with the experimental data with high accuracy, closer fitting of the velocity profile is necessary.

For the inner layer, the equation reported by Musker (1979) is well known although it is not written in this abstract. This equation represents the velocity profile of the inner layer, however, a small deviation near $y^+ = 50$ (the hump) is observed. To fit the velocity profile near $y^+ = 50$, Monkewitz et al. (2007) proposed the following equation,

$$U_i^{\ +} = U_{iM}^{\ +} + \frac{\exp\left[-\ln^2\left(y^+/d_1\right)\right]}{d_2} \tag{4}$$

where, U_{iM} is the velocity profile given by the Musker equation (1979). Monkewitz et al. (2007) proposed $d_1 = 30$ and $d_2 = 2.85$. For the boundary layer, Eq.(4) suitably represents the velocity profile shown by Chauhan et al.(2009). For the pipe flow in this experiment, d_1 and d_2 proposed by Monkewitz et al. cannot suitably represent the velocity profile data. By fitting to the velocity profile data, $d_1 = 26.5$ and $d_2 = 4.53$ are proposed in this paper.

For the outer layer, Coles (1956) proposed the wake function as follows.

$$U_o^{\ +} = \frac{1}{\kappa}\ln y^+ + B + \frac{2\Pi}{\kappa}W(\eta) \tag{5}$$

where $\eta = y/(D/2)$. Several wake functions $W(\eta)$ have been proposed in previous papers. In this paper, the following equation is used.

$$W(\eta) = b_1\eta^3 + b_2\eta^2 + b_3\eta + b_4 \tag{6}$$

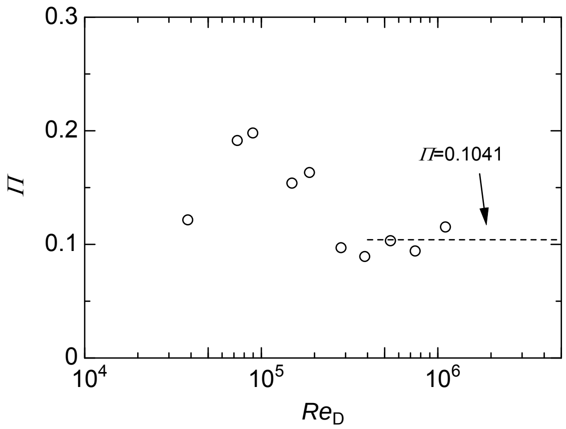

Figure 6. Variation of Π in wake function.

where b_1 = -5.907, b_2 = 8.093, b_3 = -9.856×10^{-1}, and b_4 = 1.001×10^{-4}. Assuming Eq.(6), the variation of Π is obtained from the measured velocity profile as shown in Fig.6. Similar to the behavior of the Kármán constant and the additive constant, Π also has a Reynolds number dependence. Π has a peak value of around $Re_D \approx 10^5$, and it has an almost constant value for $Re_D > 3.0\times10^5$. Π = 0.1041 is obtained as the average for $Re_D > 5.0\times10^5$.

As the final form of the velocity profile, Eq.(4) and the wake function are combined. The following fitting velocity profile is shown in Fig.3.

$$U^+ = U_i^+ + \frac{2\Pi}{\kappa} W(\eta) \tag{7}$$

This equation is shown in Fig.3 as the solid line. The fitting velocity profile suitably represents the velocity profile data except in the viscous sublayer at higher Reynolds numbers. The relative deviation of the velocity profile data from Eq.(7) to the maximum velocity is less than 0.7%.

Consistency between Velocity Profile and Friction Factor.

When the strict relation for the friction factor from the velocity profile is necessary, Musker equation should be integrated. However, the integration of it is complexed, and the consistency for the additive constant B is difficult to observe directly. By integrating the defect of the velocity given by Eq.(5), the following equation is obtained.

$$\frac{1}{\sqrt{\lambda}} = \frac{1}{2\kappa\sqrt{2}} \ln\left(Re_D\sqrt{\lambda}\right) + \frac{B}{2\sqrt{2}} - \frac{1}{2\kappa\sqrt{2}}\left\{\frac{3}{2} + \ln\left(4\sqrt{2}\right)\right\} + \frac{\Pi}{\kappa\sqrt{2}}\left(\frac{b_1}{10} + \frac{b_2}{6} + \frac{b_3}{3} + b_4\right) - C\left(Re_D\right) \tag{8}$$

where $C(Re_D)$ is the correction term for the inner layer. In this experiment, $C(Re_D)$ is estimated by the numerical integration of the difference between Eq.(2) and Eq.(4) as follows.

$$C\left(Re_D\right) = \frac{\sqrt{8}}{D^2}\int_{y^*}^{D/2}\left(U_{\mathrm{Eq4}}{}^+ - U_{\mathrm{Eq2}}{}^+\right)\left(\frac{D}{2} - y\right)dy \tag{9}$$

where $U_{\mathrm{Eq2}}{}^+$ and $U_{\mathrm{Eq4}}{}^+$ are the velocity profiles given by Eq.(2) and Eq.(4), respectively. y^* means the wall normal position where Eq.(2) and Eq.(4) cross each other in the viscous sublayer. The unintegrated region less the y^* does not influence to the result of $C(Re_D)$. Finally, the fitting curve for $C(Re_D)$ is given by the following.

$$C\left(Re_D\right) = 15614\, Re_D{}^{-1.231} \tag{10}$$

The influence of the correction to the friction factor is up to app. 4% at Re_D = 1.0×10^4. However, it decreases with the Reynolds number and is 0.02% at Re_D = 1.0×10^6. Furthermore, the influence is negligibly small at Re_D=1.0×10^7.

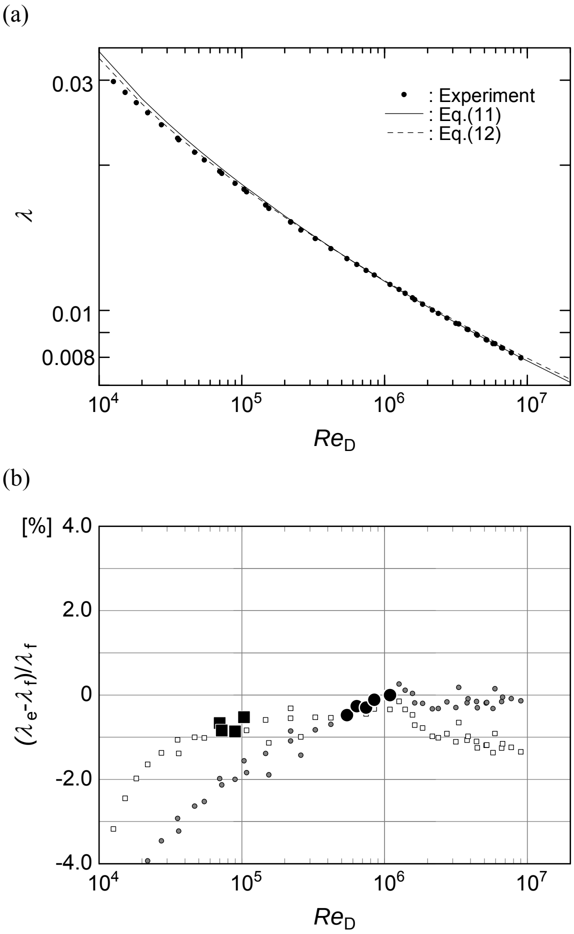

Figure 7. Difference between experimental data and Eq.(11),(12). λ_f is given by Eq.(11) for the gray circles and Eq.(12) for the white rectangle. The larger makers indicate the data used to calculate the constants.

To obtain the final form of Eq.(8), the constants κ, B, and Π are substituted. As shown in above, these constants have Reynolds number dependency. But, these values seem to be constant for $Re_D > 5.0\times10^5$. If these constants do not change over the examined Reynolds number range, which is $Re_D > 1.1\times10^6$, the equation using them is expected to represent the friction factor data. Substituting the constants $\kappa = 0.383$, $B = 4.335$, and $\Pi = 0.1041$ and Eq.(10), the following equation is given.

$$\frac{1}{\sqrt{\lambda}} = 2.126\log\left(Re_D\sqrt{\lambda}\right) - 1.361 - 15614\,Re_D^{-1.231} \quad (11)$$

It should be noted that Eq.(11) is the relationship for the friction factor completely obtained by the mean velocity profile data. Equation (11) is drawn in Fig.7(a), and the difference between Eq.(11) and the friction factor data at the Hi-Reff is shown in Fig.7(b). λ_e is the experimental data and λ_f is the friction factor given by Eq.(11). The difference between Eq.(11) and the friction factor data is from –0.48% to –0.04% for the range of $5.4\times10^5 < Re_D < 1.1\times10^6$, as shown by the larger markers. This result shows that the friction factor derived by the mean velocity profile data is highly consistent with the friction factor data. Furthermore, for Reynolds numbers larger than 1.1×10^6, the differences between Eq.(11) and the friction factor data are almost constant at –0.33% to 0.26%. The average deviation for $5.4\times10^5 < Re_D < 1.0\times10^7$ is –0.14%.

On the other hand, for lower Reynolds numbers $Re_D < 5.4\times10^5$, Eq.(11) is not consistent with the friction factor data. This inconsistency is caused by the constants being different between higher and lower Reynolds numbers. Although those constants have Reynolds number dependency, the average value for the low Reynolds number region $8.0\times10^4 < Re_D < 1.0\times10^6$ is used to derive the equation for the friction factor. The constants are $\kappa = 0.395$, $B = 4.785$, and $\Pi = 0.1945$, and the following equation is given:

$$\frac{1}{\sqrt{\lambda}} = 2.077\log\left(Re_D\sqrt{\lambda}\right) - 1.096 - 15614\,Re_D^{-1.231} \quad (12)$$

This equation is also shown in Fig.7(a) and (b). Equation (12) is clearly closer to the friction factor data than Eq.(12), especially at low Reynolds numbers. In Fig. 7(b), the deviations in the Reynolds number ranges mentioned above are emphasized by the larger markers. The deviation of the friction factor data from Eq.(12) for this Reynolds number range is app. –0.7%. Furthermore, Eq.(12) represents the friction factor data of less than 1% up to $Re_D = 2.0\times10^6$. However, for higher Reynolds numbers, the deviation has Reynolds number dependency. With an increase in the Reynolds number, the deviation increases. This shows that the constants for Eq.(12) are not consistent with the fluid mechanics of pipe flow at higher Reynolds numbers.

Best Fitting to Friction Factor Data.

In the previous sections, the relationship between the friction factor and Reynolds number is obtained by the velocity profile data. The friction factor obtained from the velocity profile data is consistent with the friction factor data at the Hi-Reff. This means that both measurements at the Hi-Reff are performed with high accuracy and reliability. In this section, the constants in the equations for the friction factor given in the previous section are obtained by fitting to the friction factor data at the Hi-Reff. However, since the constants have Reynolds number dependency, it is difficult to apply them for a wide range of Reynolds numbers. When the equation is derived according to the correct fluid mechanics in the pipe, the relationship between the friction factor and Reynolds number cannot represent a unique equation for $Re_D > 1.0\times10^4$. McKeon et al. (2005) suggest that the friction factor behavior falls into three regimes of Reynolds numbers: $Re_D < 1.0\times10^5$, $1.0\times10^5 < Re_D < 3.0\times10^5$, and $Re_D > 3.0\times10^5$ (although they express them with unique equations). The criteria around $Re_D = 3.0\times10^5$ is also found in the results at the Hi-Reff, as shown in the results of the velocity profile based on log law. The constants for the log law have Reynolds number dependency for $Re_D < 3.0\times10^5$, and they are constant for $Re_D > 5.0\times10^5$. In this section, the coefficients are estimated for different Reynolds number ranges to observe the Reynolds number dependency.

The friction factor data is fitted to Eq.(7), and the constants κ, B, and Π are determined. The influence of the inner layer is given by Eq.(9). The obtained constants are shown in Table 1 for different Reynolds number ranges. Depending on the Reynolds number range, the constants are varied. The result is roughly classified into two

Table 1. Constants for variable Reynolds number range

Data source	Re_D from	Re_D to	κ	B	Π	C
Friction factor	1.2×10^4	3.3×10^5	0.404	5.455	0.102	-0.871
	1.2×10^4	1.0×10^6	0.402	5.383	0.102	-0.911
	1.2×10^4	1.0×10^7	0.394	5.082	0.099	-1.075
	3.3×10^5	1.0×10^7	0.384	4.450	0.099	-1.375
	5.5×10^5	1.0×10^7	0.383	4.386	0.099	-1.405
	1.5×10^6	1.0×10^7	0.384	4.417	0.099	-1.391
Velocity profile	5.5×10^5	1.0×10^6	0.383	4.335	0.104	-1.361

regions with a boundary of Re_D = 3.0×10^5. When the Reynolds number range includes Re_D < 3.0×10^5, the Kármán constant is from app. 0.39–0.40. It should be noted that the results in the first and second rows in Table 1 are similar to the constants of the Prandtl equation. On the other hand, when the Reynolds number range does not include Re_D < 3.0×10^5, the Kármán constant is app. 0.385, as shown in the fourth and fifth rows. Such result behaviors show the consistency with the result of the velocity profile data, as shown in Figs.2 and 3.

As the best fitting for friction factor data at a wide range of Reynolds numbers, the following equation is proposed using the constants on the third row in Table 1.

$$\frac{1}{\sqrt{\lambda}} = 2.064\log\left(Re_D\sqrt{\lambda}\right) - 1.025 - 15614\,Re_D^{-1.231} \quad (13)$$

This equation represents the friction factor data from –0.83% to 0.77% for 1.8×10^5 < Re_D < 1.0×10^7. However, it should be noted that the constants do not reflect the actual constants in the velocity field of the pipe.

CONCLUSION

The new measurement data of the friction factor and the velocity profile in a smooth pipe at the Hi-Reff was obtained at high Reynolds numbers up to 10^7 with high accuracy. Using the experimental data, the relation between the friction factor and the velocity profile was discussed in detail in this paper.

The consistency between the velocity profile and the friction factor is investigated by integrating the velocity profile data. The velocity profile data is fitted to the log law, and the equation for the friction factor is derived by the integration of the fitted velocity profile. The equation obtained suitably represents the friction factor data. The deviation of the equation from the friction factor data is less than 1%. By this analysis, it is indicated that the friction factor for 10^4 < Re_D < 10^7 cannot be expressed by a unique equation of the velocity profile based on the log law because the Kármán and additive constants have Reynolds number dependencies at low Reynolds numbers, Re_D < 3×10^5. For larger Reynolds numbers, Re_D > 5×10^5, the friction factor can be expressed by a unique equation, which yields κ = 0.383 and B = 4.335.

Based on the equation form given by the velocity profile, the best fitting constants for the friction factor data are proposed. For the lower Reynolds number region 1.2×10^4 < Re_D < 1.0×10^6, the Kármán constants and the constant C are roughly similar to the Prandtl equation values, which are κ = 0.402 and C = –0.911. For the higher Reynolds number region 5.5×10^5 < Re_D < 1.0×10^7, they are estimated as κ = 0.383 and C = –1.405, which yield B = 4.386. Those values are in good agreement with the constants obtained from the velocity profile data. The equation shows that the friction factor data is less than 0.8%.

REFERENCES

Chauhan, K. A., Monkewitz, P. A., and Nagib, H. M., 2009, "Criteria for assessing experiments in zero pressure gradient boundary layers", *Fluid Dynamic Research*, 41, 021404

Coles, D. E., 1956, "The law of the wake in the turbulent boundary layer" *J. Fluid Mech.*, 1, 191–226

den Toonder, J. M. J., and Nieuwstadt, F. T. M., 1997 "Reynolds number effect in a turbulent pipe flow for low to moderate Re", *Physics of Fluids*, 9(11), 3398-3409

Furuichi, N., Sato, H., Terao Y., and Takamoto, M., 2009, "A New Calibration Facility of Flowrate for High Reynolds Number", *Flow Meas. Inst.* 20-1, 38-47

Furuichi, N., Terao, Y., Wada Y. and Tsuji Y., "Friction factor and mean velocity profile for pipe flow at high Reynolds numbers", *Physics of Fluids*, 27, 095108 (2015), DOI: 10.1063/1.4930987

McKeon, B. J., Swanson, C. J., Zagarola, M. V., Donnelly, R. J., and Smits, A. J., 2004 "Friction factors for smooth pipe", *J. Fluid Mech.* 511, 41-44

McKeon, B. J., Zagarola M. V., and Smits, A. J., 2005, "A new friction factor relationship for fully developed pipe flow", *J. Fluid Mech.* 538, 429-443

Monkewitz P A, Chauhan K A and Nagib H M 2007 Self-consistent high-Reynolds number asymptotics for ZPG turbulent boundary layers Phys. Fluids 19 115101

Monty, J. P., 2005 "Developments in smooth wall turbulent duct flows," Ph.D. thesis, University of Melbourne, Australia.

Musker, A. J., 1979, "Explicit expression for the smooth wall velocity distribution in a turbulent boundary layer", *AIAA J.*, 17, 655–7

Nagib, H. M., and Shauhan, K. A., 2008, "Variations of von Kármán coefficient in canonical flows", *Physics of Fluids*, 20, 101518, DOI: 10.1063/1.3006423

Nikradse, "Laws of turbulent flow in smooth pipes", NASA TT F-10, 1932 (English translation; 1966)

Zagarola, M. V., and Smits, A. J., 1998 "Mean-flow scaling of turbulent pipe flow", *J Fluid Mech.* 373, 33-79